Improvement of graphene quality synthesized by cluster ion implantation

Z.D. Zhang [a], Z.S. Wang [a], R. Zhang [a], X.Y. Wu [b], D.J. Fu [a,*], J.R. Liu [a]

[a] School of Physics and Technology and Key Laboratory of Artificial Micro- and Nano-Materials of Ministry of Education, Wuhan University, Wuhan 430072, China
[b] Key Laboratory of Beam Technology and Material Modification of Ministry of Education, Beijing Normal University, Beijing 100875, China

ABSTRACT

Graphene was prepared by negative C_4 cluster ion implantation at 5 keV/atom followed by vacuum thermal annealing and cooling. The surface morphology and structure of samples were studied by scanning electron microscopy, atomic force microscopy, and Raman spectroscopy. Improvement of the graphene quality was realized by optimization of the post thermal processes. 1–2 layer graphene was obtained with I_{2D}/I_G ratio of 1.43 and I_D/I_G ratio of 0.07 at the implantation dose of 12×10^{15} atoms/cm^2 and annealed at 900 °C followed by cooling at 20 °C/min.

© 2013 Elsevier B.V. All rights reserved.

Since the discovery of single-layer graphene in 2004 [1], graphene has attracted intensive interest due to its two dimensionality and unique properties, including quantum spin Hall effect [2], phase-coherent transport [3], bipolar supercurrent [4], suppression of weak localization [5], and deviation from the adiabatic Born–Oppenheimer approximation [6]. The unique structure and properties of graphene make it a promising for a wide variety of new technological applications [7–9], such as graphene-based composites, supercapacitors, batteries, fuel cells, conductive pads and inks, flexible touch screen displays, generic intelligent coatings, and sensors. Up to now graphene has been prepared by many methods, such as mechanical exfoliation of graphite, thermal decomposition of SiC, chemical vapor deposition (CVD), and molecular beam epitaxy. Garaj et al. [10] and Baraton [11] used ion implantation technology to introduce a precise dose of carbon atoms Ni films and obtained graphene by subsequent precipitation of carbon on Ni surface upon heat treatment. Recently Zhang et al. prepared few-layer graphene by using negative C_1–C_4 cluster ion implantation and found that nonlinear radiation effect of the carbon cluster ions and lower implant energy had significant influence on the graphene quality [12,13]. In this letter, we report on formation of 1–2 layer graphene with lower defect density and large area coverage by the negative ion beam process using the specific C_4 clusters.

The graphene samples were prepared by cluster ion implantation using 20 keV negative C_4 cluster ion beams produced from a SNICS (source of negative ion by cesium sputtering) source. The ion beam was scanned with electrostatic X- and Y-scanners to meet the demand for uniformity of the ion implantation. The substrates were 300 nm-thick Ni films deposited by e-beam evaporation on 300 nm SiO$_2$ layers formed via thermal oxidation of Si wafers. The small negative carbon clusters C_4 were implanted at 20 keV to doses of 8×10^{15} atoms/cm^2, 12×10^{15} atoms/cm^2, and 16×10^{15} atoms/cm^2, which correspond to 2, 3, and 4 graphene layers, respectively. Then the samples were placed in a quartz boat in the furnace for thermal annealing and cooling. The surface morphology of the graphene samples was investigated by scanning electron microscope (SEM, JSM-6700F JEOL) and atomic force microscope (AFM, SHMADZUSPM-9500J3). The chemical bonding of the samples was characterized on an RM-1000 Confocal Raman spectrometer in backscattering geometry excited by an Ar laser at a wavelength of 514.5 nm.

Fig. 1(a–c) shows SEM images of the synthesized graphene on the Ni films implanted with various carbon doses. X-ray diffraction confirmed that the Ni films for the implantation had predominant (1 1 1) orientation. The cluster ion implantation was conducted at the same energy (20 keV) and the annealing was performed by dwelling at 900 °C for 50 min and subsequent cooling to room temperature at a rate of 20 °C/min in vacuum. The cluster ion energy of 20 keV can be expressed as 5 keV/atom and the projected range calculated by the SRIM (stopping and range of ions in matter) code is less than 6.5 nm [12], approximately 2.2% of the total thickness of the Ni films. The cluster–solid interaction takes place in an ultra-shallow surface layer ensures diffusion of carbon atoms to form a thin graphene layer at the top surface. In Fig. 1 the grain boundaries of Ni are observed as gray color, while the dark area is identified as the SiO$_2$ substrate. With increasing dose, the precipitated graphene becomes more uniform and larger in area over the whole Ni surface.

* Corresponding author. Tel./fax: +86 27 6875 3587.
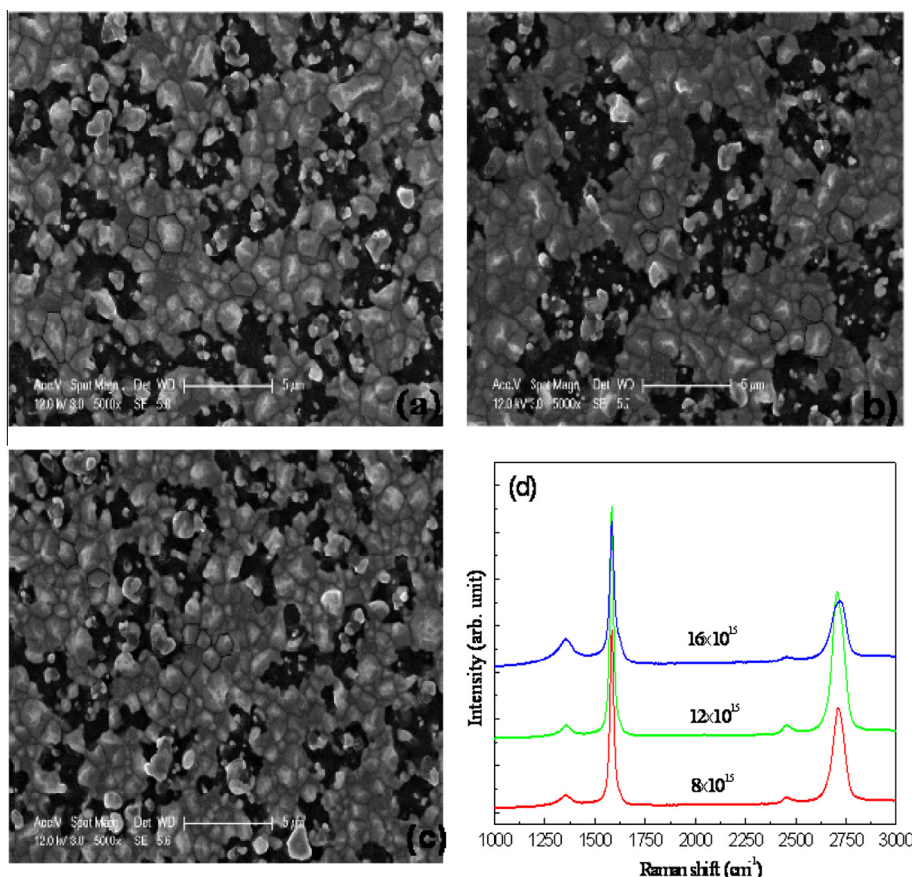 *E-mail address:* djfu@whu.edu.cn (D.J. Fu).

Fig. 1. (a–c) SEM images of C_4 cluster ion implanted Ni films to doses of 8×10^{15}, 12×10^{15}, and 16×10^{15} atoms/cm^2 and (d) Raman spectra of graphene with different carbon dosages annealed at 900 °C for 50 min followed by cooling to room temperature at 20 °C/min.

Fig. 1(d) shows Raman spectra of the samples with carbon doses of 8×10^{15} atoms/cm^2, 12×10^{15} atoms/cm^2, and 16×10^{15} atoms/cm^2, respectively. The I_D/I_G ratios are 0.09, 0.07, and 0.22, indicating presence of rather few defects. In particular, the spectra reveal that the sample with carbon dose of 12×10^{15} atoms/cm^2 exhibits a surface layer of low defect graphene. The equivalent of 2, 3 and 4 graphene layers should be formed, respectively, assuming a uniform precipitation of the total implanted C at the surface of the Ni film. However, the I_{2D}/I_G ratios are 0.57, 0.64, and 0.47, respectively, mean that the thicknesses of the measured area are 3 graphene layers for all the three samples. It is possible that the precipitation of the implanted C is not uniform and the amount of precipitated carbon cannot be controlled only by the implant dose.

The major requirement in preparation of graphene layer with high area coverage is the well controlled amount of carbon density and the uniformity. Compare with CVD and other techniques, ion implantation is the most quantitatively controllable process. The volume density of C in transition metal films is controlled by implantation dosage with the accuracy up-to 1–2%. The area uniformity in ion implantation with good scanning is about 1–2%. The new problem is the energetic ion induced damage in the transition metal films, like polycrystalline Ni film. At the C ion implantation dosage for n layer graphene synthesis, $n \times 3.8 \times 10^{15}$ C/cm^2, the shallow ion implantation does perturb crystalline grain structure of a metallic substrate. In the case of C-cluster ion implantation this irradiation process even more complicated due to the non-linear effect in cluster induced damage and cluster induced sputtering [14]. Recently, Zhang et al. observed the favorable effect

of C-cluster ion implantation in graphene synthesis. The Raman spectroscopy study of the graphene layers shows reduced disorders due to the non-linear effect in cluster-solid interaction. AFM scanning of the graphene layer shows better surface smoothness due to the enhanced non-linear sputtering effect in C-cluster implantation. These two positive effects in C-cluster ion implantation, the reduced disorders and the improved smoothness, will be essential factors in synthesis of large area graphene films with high area coverage.

Fig. 2 shows Raman spectra and mapping result of graphene which was prepared by C_4 ion implantation with a dosage of 12×10^{15} atoms/cm^2 at 20 keV under the annealing process of dwelling at 900 °C for 60 min before cooling the sample to room temperature at a rate of 30 °C/min in high vacuum. The small D peak at 1354 cm^{-1} arising from symmetry-breaking features, such as graphene defects and domain boundaries, a strong G peak at 1583 cm^{-1} associated with sp^2 C-bond stretching, a 2D peak at 2712 cm^{-1} emerging from a double resonant scattering phenomenon [15]. The I_D/I_G ratio of 0.55 indicates the existence of a large density of defects in the graphene and I_{2D}/I_G ratio of 0.51 indicates 3–4 layers graphene. Raman mapping was conducted over an area of 10×10 μm^2 of the sample. The mapping images of the G peak, 2D peak and G/2D ratio are shown in Fig. 2(b–d). The G/2D ratio mapping show that 70% coverage of the surface is 3 + L layer graphene, and monolayer and bilayer graphene have been obtained on 30% area of the surface. It is further demonstrated that the non-uniformity of the carbon density at the surface is significantly dependent on the precipitation process. Some carbon atoms might precipitate at the Ni-SiO$_2$ interface or be trapped at the Ni grain
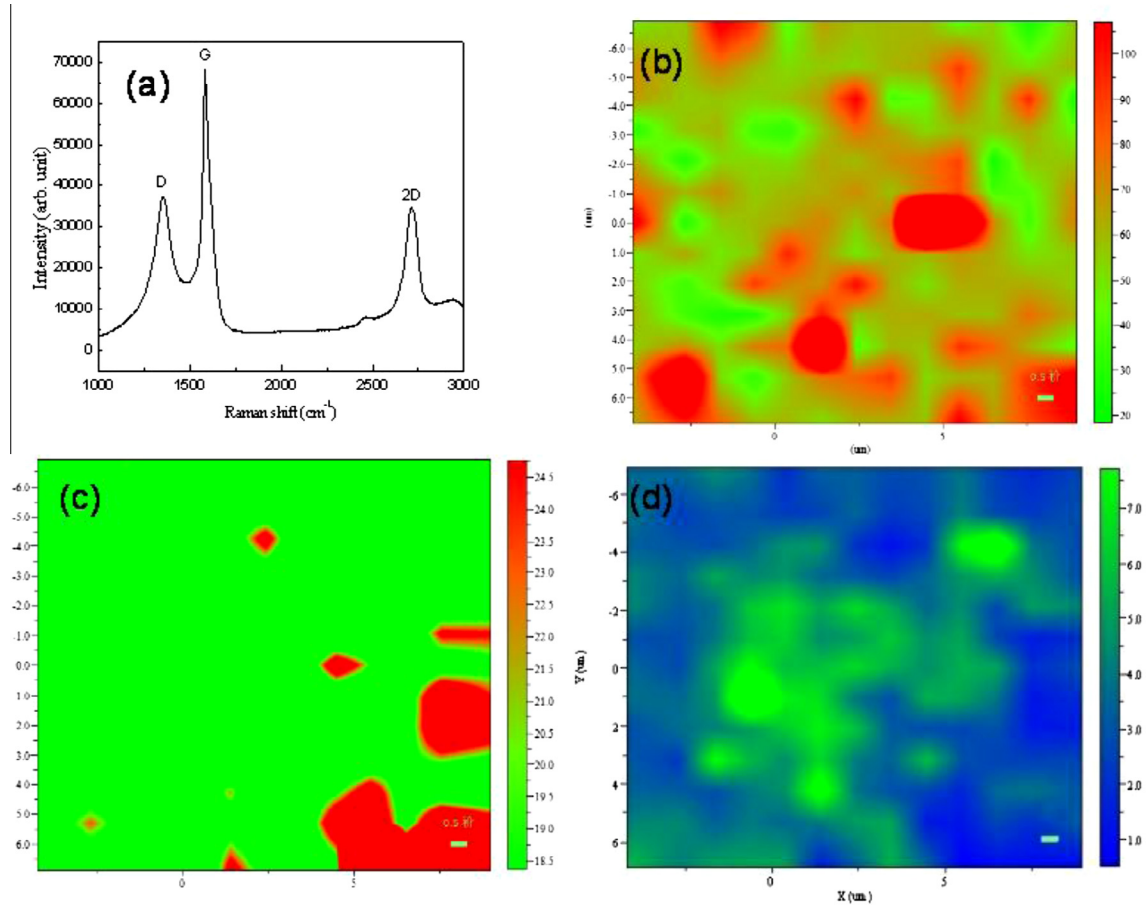
Fig. 2. (a) Raman spectra of the graphene prepared with post-implantation annealing at 900 °C for 60 min followed by cooling to room temperature at 30 °C/min and mapping (b) G band intensity; (c) 2D band intensity; (d) G/2D ratio mapping.

boundaries upon thermal treatment. These factors affect the uniformity of graphene and the discrepancy between the thickness of graphene measured and that expected from the implant dose.

To elucidate the effect of the subsequent thermal annealing and cooling parameters on graphene growth and uniformity, three thermal-treatment schemes were performed, as shown in Fig. 3(a). Briefly, the samples were kept at 900 °C for 50–60 min in vacuum and then slowly cooled down to room temperature at a rate of 20 °C/min or 30 °C/min. This high temperature allows carbon atoms to dissolve in Ni, while different cooling rates result in distinct precipitation rates. As the solubility of carbon in the Ni film decreases with decreasing temperature, the carbon atoms diffuse to the surface and form graphene. Previously, Zhang et al. [13] used different thermal schemes: via annealing at 900 °C for 50 min followed by cooling to 725 °C at different rates and quenching to study the non-linear radiation effect in graphene synthesis. The results suggest that a moderate cooling rate is necessary for thin layer graphene formation.

Fig. 3(b) shows Raman spectra of graphene prepared by C_4 ion implantation with doses of 8×10^{15} atoms/cm^2, 12×10^{15} atoms/cm^2 and 16×10^{15} atoms/cm^2, and post-treated under three different schemes. It is seen that when the dwelling time at 900 °C remains 60 min, but the cooling rate is decreased from 30 °C/min to 20 °C/min, the I_D/I_G ratios decrease from 0.51, 0.55 and 0.33 to 0.05, 0.07 and 0.07, respectively, for the three samples with different carbon doses, indicating better out-diffusion of C atoms. However, the I_{2D}/I_G ratio which represents the thickness of graphene does not change much except at the dose of 12×10^{15} atoms/

cm^2. At this dose, as the cooling rate decreases, the I_{2D}/I_G ratio increases from 0.51 to 1.43, indicating formation of 1–2 layer graphene. When the dwelling duration at 900 °C shorten from 60 min to 50 min, with the cooling rate (20 °C/min) and the other parameters being fixed, the thickness of graphene was not changed. Few defects are introduced, since the samples have the low I_D/I_G ratio of 0.09, 0.07 and 0.22. These results demonstrate that it is the cooling rate rather than the dwelling duration that affects the amount of carbon segregated at Ni surface and quality of graphene formed. The lower cooling rate 20 °C/min is preferable to 30 °C/min for the carbon atoms to rearrange and self-heal its topological defects and for the growth of thinner layer graphene with fewer defects and monolayer and bilayer graphene coverage may be increased at this cooling rate. In fact, at faster cooling rates, a significant amount of carbon atoms segregate at the surface within short time; they may not have sufficient time to reach states needed for good crystallization. As a result, thicker layer graphene or graphite with large amount of defects and inhomogeneity would be formed.

It has been observed that the Ni grain boundaries are energetically favorable for carbon segregation and precipitation [15]. The formation of multilayer graphene can be attributed to the enhanced carbon segregation localized at polycrystalline grain boundaries, while the formation of bilayer and monolayer graphene is mainly observed on the flat central areas of large crystalline grains [16]. Namely, 1–2 layer regions consisting of micrometer-sized graphene domains are distributed over the flat area of large Ni grains, and the thicker 3 + L regions are mostly located at the
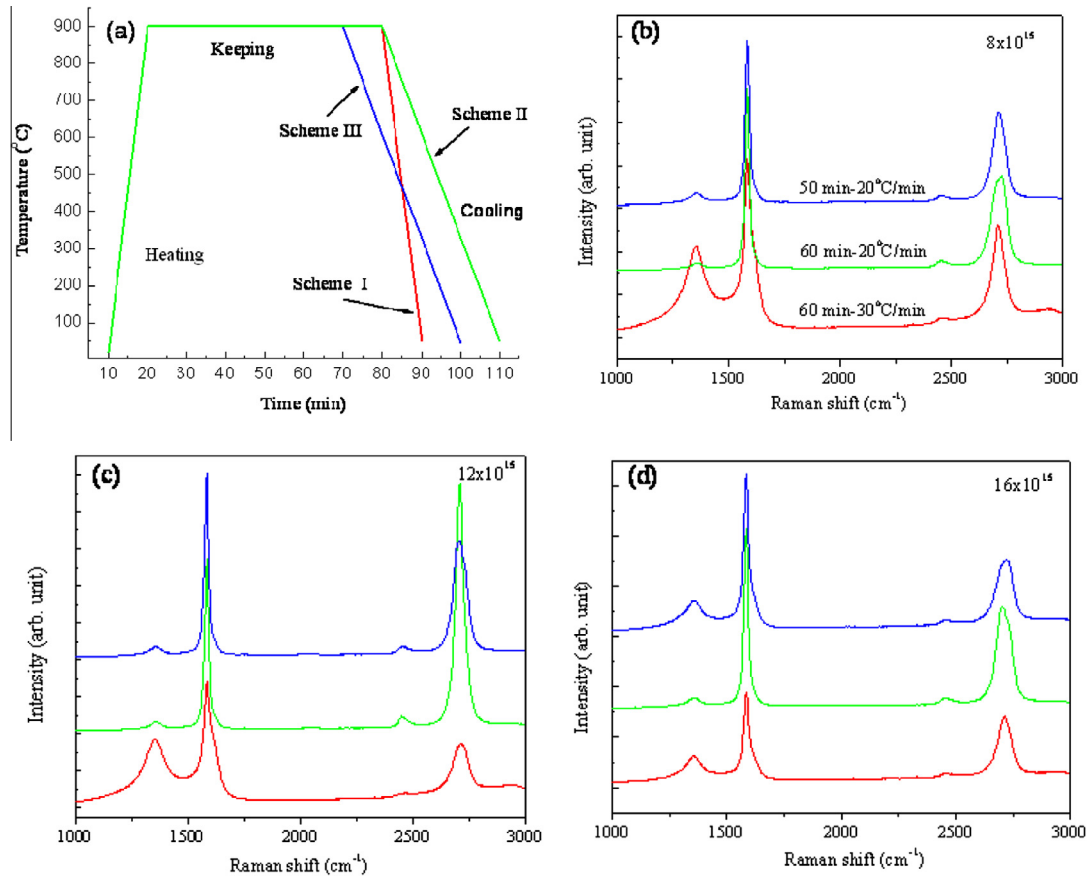
Fig. 3. (a) Thermal treatment schemes for the graphene prepared by C$_4$ cluster ion implantation and (b–d) Raman spectra of graphene prepared by C$_4$ cluster implantation with different dosages and annealed following different schemes.
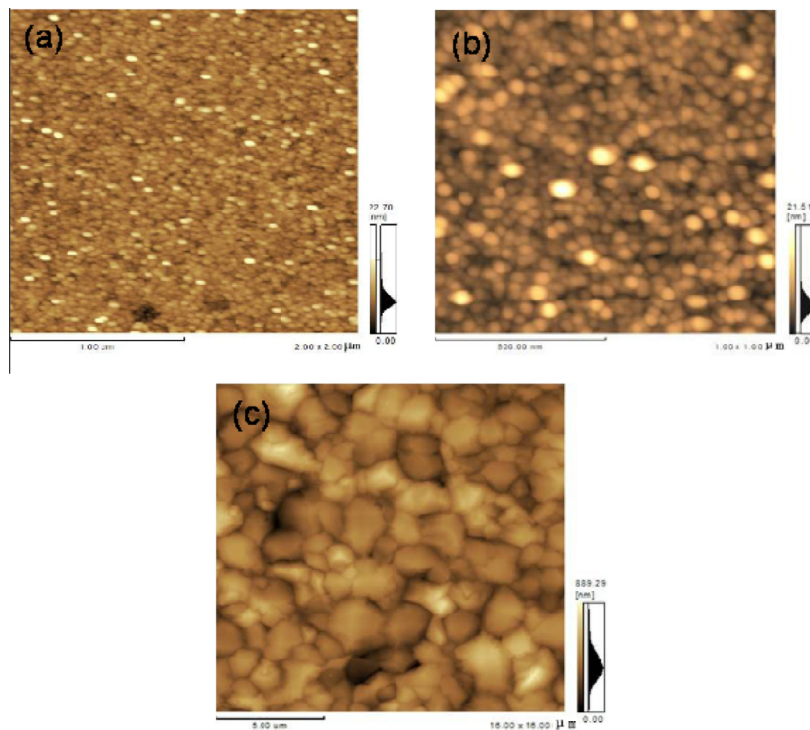

Fig. 4. AFM surface morphologies of the Ni film and graphene: (a) Ni film before implantation; (b) Ni film after implantation; (c) graphene prepared by ion implantation and subsequent thermal processing.

grain boundaries. Therefore, there is a close correlation between the grain size distributions and surface homogeneity of the polycrystalline Ni film and the morphology of the graphene films [17].

To maximize the monolayer and bilayer coverage and improve the uniformity, it is necessary to investigate variation of the surface morphology and grain size of the Ni films upon cluster ion implantation. Fig. 4(a and b) show AFM images of the Ni films before and after implantation. The root-mean-square roughness of the samples is 2.6 nm and 2.21 nm, respectively, indicating that the surface of Ni film is smoother and more uniform after C-cluster ion implantation. This means that the grain structure and the surface morphology of the polycrystalline Ni film were changed by the cluster-induced damage and surface sputtering. In particular, the nonlinear enhanced sputtering effect of the cluster ions induces surface smoothing of the Ni substrate [13]. Fig. 4(c) shows the AFM image of graphene prepared with 12×10^{15} carbon/cm^2 annealed at 900 °C for 60 min and cooled at 20 °C/min to room temperature. Graphite flakes and few-layer graphene are seen on the surface of the Ni film with large grains. The large-size graphene domains are attributed to the growth of Ni grain during annealing.

In conclusion, we have prepared graphene on Ni films by negative C_4 cluster ion implantation followed by thermal annealing and cooling. The implantation was conducted with 8×10^{15}–16×10^{15} atoms/cm^2 on polycrystalline Ni (1 1 1) films with grain size of 20–30 nm. Raman spectroscopy and mapping measurements showed that the number of graphene sheets and density of defects were influenced by the amount of precipitated carbon and cooling rate. 1–2 layer graphene was obtained with I_{2D}/I_G ratio of 1.43 and I_D/I_G ratio of 0.07 at the implantation dose of 12×10^{15} atoms/cm^2 and annealed at 900 °C followed by cooling at 20 °C/min. The surface of Ni film is smoother and more uniform after C-cluster ion implantation with the rms roughness decreasing from 2.6 nm to 2.21 nm. Ni grains grow during annealing, and larger Ni grain sizes are favorable for the formation of thinner layer graphene regions. The thickness uniformity of the graphene layer can be further improved by fine tuning of the cooling parameters.

Acknowledgments

References

[1] K.S. Novoselov, A.K. Geim, S.V. Morozov, D. Jiang, Y. Zhang, S.V. Dubonos, I.V. Grigorieva, A.A. Firsov, Science 306 (2004) 666.
[2] Y.B. Zhang, Y.B. Tan, H.L. Stomer, P. Kim, Nature 438 (2005) 201.
[3] F. Miao, S. Wijeratne, Y. Zhang, U.C. Coskun, W. Bao, C.N. Lau, Science 317 (2007) 1530.
[4] H.B. Heersche, P. Jarillo-Herrero, J.B. Oostinga, L.M.K. Vandersypen, A.F. Morpurgo, Nature 446 (2007) 56.
[5] S.V. Morozov, K.S. Novoselov, M.I. Katsnelson, F. Schedin, L.A. Ponomarenko, D. Jiang, A.K. Geim, Phys. Rev. Lett. 97 (2006) 016801.
[6] S. Pisana, M. Lazzeri, C. Casiraghi, K.S. Novoselov, A.K. Geim, A.C. Ferrari, F. Mauri, Nat. Mater. 6 (2007) 198.
[7] C. Berger, Z. Song, T. Li, X. Li, A.Y. Ogbazghi, R. Feng, Z. Dai, A.N. Marchenkov, E.H. Conrad, P.N. First, W.A. de Heer, J. Phys. Chem. B 108 (2004) 19912.
[8] F. Schedin, A.K. Geim, S.V. Morozov, E.W. Hill, P. Blake, M.I. Katsnelson, K.S. Novoselov, Nat. Mater. 6 (2007) 652.
[9] B. Trauzettel, D.V. Bulaev, L. Loss, G. Burkard, Nat. Phys. 3 (2007) 192.
[10] S. Garaj, W. Hubbard, J.A. Golovchenk, Appl. Phys. Lett. 97 (2010) 183103.
[11] L. Baraton, Z.B. He, C.S. Lee, J.L. Maurice, C.S. Cojocaru, A.F. Gourgues- Lorenzon, Y.H. Lee, D. Pribat, Nanotechnology 22 (2011) 085601.
[12] Z.S. Wang, Z.D. Zhang, R. Zhang, S.X. Wang, D.J. Fu, J.R. Liu, Chinese Sci. Bull. 27 (2012) 3556.
[13] R. Zhang, Z.D. Zhang, Z.S. Wang, S.X. Wang, D.J. Fu, J.R. Liu, Appl. Phys. Lett. 101 (2012) 011905.
[14] H.H. Andersen, H.L. Bay, J. Appl. Phys. 45 (1974) 953.
[15] A.C. Ferrari, J.C. Meyer, V. Scardaci, C. Casiraghi, M. Lazzeri, F. Mauri, S. Piscanec, D. Jiang, K.S. Novoselov, S. Roth, A.K. Geim, Phys. Rev. Lett. 97 (2006) 187401.
[16] S. Thiele, A. Reina, P. Healey, J. Kedzierski, P. Wyatt, P.L. Hsu, C. Keast, J. Schaefer, J. Kong, Nanotechnology 21 (2010) 015601.
[17] A.T.S. Reina, X. Jia, S. Bhaviripudi, M.S. Dresselhaus, J.A. Schaefer, J. Kong, Nano Res. 2 (2009) 509.